ISSN 2075-1133, Inorganic Materials: Applied Research, 2018, Vol. 9, No. 1, pp. 1–8. © Pleiades Publishing, Ltd., 2018.
Original Russian Text © M.S. Belyayev, V.F. Terentyev, M.A. Gorbovets, M.M. Bakradze, O.S. Antonova, 2017, published in Materialovedenie, 2017, No. 3, pp. 18–24.

Low-Cycle Fatigue under Controlled Deformation and Fracture of the Superalloy VZh175

M. S. Belyayev[a, *], V. F. Terentyev[b], M. A. Gorbovets[a], M. M. Bakradze[a], and O. S. Antonova[b]
[a]*All-Russian Scientific Research Institute of Aviation Materials, VIAM, Moscow, Russia*
[b]*Baikov Institute of Metallurgy and Materials Science, Russian Academy of Sciences, Moscow, Russia*
**e-mail: bms-oti@mail.ru*
Received April 26, 2016

Abstract—Low-cycle fatigue of the superalloy VZh175 heat-resistant alloy was studied under controlled deformation at room and high temperatures. The parameters of cyclic elastoplastic deformation and characteristics of fatigue strength were considered. The peculiarities of nucleation and development of low-cycle fatigue cracks were studied.

Keywords: low-cycle fatigue, elastoplastic deformation, fractography of fractured surfaces, test temperature, VZh175 alloy

DOI: 10.1134/S2075113318010033

INTRODUCTION

The study of resistance to low-cycle fatigue (LCF) is carried out for structural materials subjected to fatigue loading in the process of operation. LCF is one of the main strength characteristics for heat-resistant materials [1–4]. Low-cycle fatigue at controlled deformation simulates to a certain extent the operational loading with small plastic deformation, and the number of loading cycles is 10^4–10^5 c. Such conditions are implemented, for example, in the parts of the rotor of gas turbine engines when exposed to high temperatures.

Change in elastoplastic deformation parameters, such as resulting stresses and amount of accumulated deformation, takes place during test for LCF under controlled deformation. Study of these parameters for different superallos, depending on the effects of temperature and deformation conditions, is of scientific and practical interest. They are usually conducted along with the determination of LCF strength characteristics and characteristics of the scatter of the experimental results, in particular. In our country, despite a number of investigations [5–7], there is a lack of such information for alloys used in high-tech industries. Investigations in this direction are widely carried out abroad [8–12].

Study of the nature of the fatigue failure allows associating its features with the loading conditions of material. The ultimate goal of such studies is ensuring the safe operation of structural components made of advanced superallos.

The parameters of elastoplastic deformation and characteristics of LCF advanced nickel VZh175 alloy at room and operating temperatures were studied in the present work. Fractographic study of the nature of fatigue fracture was conducted. The work was performed within the framework of the comprehensive scientific field 2.2. "Qualifications and Study of Materials" ("Strategic Directions of Development of Materials and Technologies of Their Processing for the Period until 2030") [2].

MATERIALS AND METHODS

High-strength nickel-based superalloy VZh175 is designed for operation at high temperatures and substantial mechanical loads as the rotor parts of aircraft GTE. It is a complex alloyed, dispersion-hardening alloy which is hardened by the intermetallic γ' phase composed of $(Ni, Co, Cr)_3$ (Al, Ti, Nd, Mo, W, V) and carbide and boride phases of different morphologies. The quantity of the hardening γ' phase is 53% [13–18].

The alloy has a complex chemical and phase composition whereupon it is hard deformed. The production technology of semifinished product includes ingot smelting by the method of double vacuum remelting, multistage thermomechanical processing, and quenching from the two-phase region with subsequent aging. It provides the optimal formation of a homogeneous fine-grained structure (Fig. 1). The alloy is characterized by high strength and plastic characteristics at room and operating temperatures (Table 1).

The LCF tests were conducted on an LFV-100 servo-hydraulic machine under control of full (elastic and plastic) deformation ε. Smooth cylindrical speci-

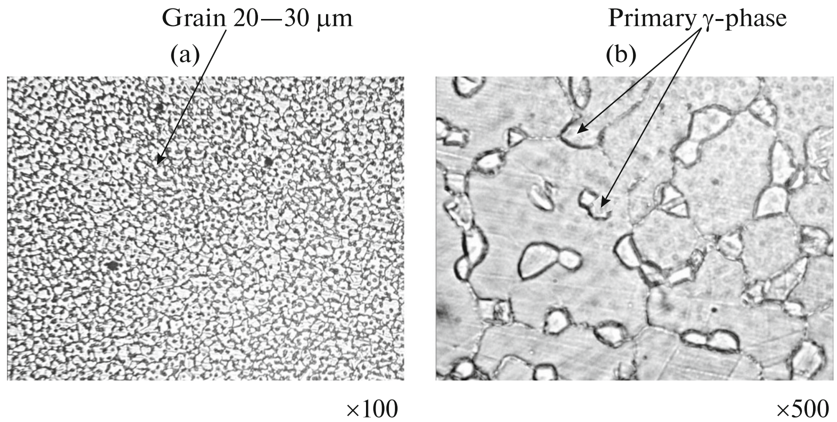

Fig. 1. Microstructure of the VZh175 superalloy: (a) (×100); (b) (×500).

mens with a diameter of 5.0 and length of 15 mm at a frequency of 1 Hz were tested. The amplitude deformation cycle LOW a was accepted as a test parameter. Recording of the loops of elastoplastic hysteresis was conducted. Tests were performed under symmetrical tension–compression cycle $R = -1$ at 20, 650, and 750°C. Tests at asymmetric cycle of deformation $R = 0$ were carried out at 650°C. The nature of fatigue fracture was investigated using TESCAN VEGA\\SB scanning electron microscope.

RESULTS AND DISCUSSION

The change in stresses in samples under given fixed deformation is shown in Fig. 2. The curves of changes in tensile–compression stresses obtained under quite near conditions to the magnitude of a given strain and number of cycles to failure of samples are presented.

The results show that, at a symmetrical cycle of deformation $R = -1$, the test temperature growth from ambient to 750°C does not change the nature of the dependence of the stress cycle. The diagram of stress changes consists of three main sections. Getting to the predetermined conditions takes place in the first section, approximately 100 cycles. The steady-state test regime with the gradual variation of tension and compression stresses implemented within approximately 0.7 N_f (N_f is the number of cycles to failure of the sample) is established in the second section. Reduction of tensile and compression stresses up to the failure of the sample takes place in the third section. The maximum stress range is achieved at given maximum amplitude of deformation and it reaches ±1200 MPa.

Analysis of experimental data shows that, in the range of $N = 2 \times 10^2$–1.5×10^4 cycles at any fixed durability, the increase in test temperature from 20 to 650 and 750°C leads to decrease in the applied deformation and appearance stresses. For example, while maintaining the general character of the stress changes at 750°C they show a slight reduction in comparison with the values at 650°C under similar values for a given deformation and number of cycles to failure N_p (Table 2). It appears that this decrease is caused by an overall softening of the alloy with the increase in the test temperature.

The influence of asymmetry of the applied deformation on the parameters of the elastoplastic hysteresis loop is considered at the temperature of 650°C when comparing the symmetric cycle $R = -1$ and cycle $R = 0$. At the asymmetric cycle of deformation $R = 0$, the shape of the stress cycle in the sample depends on the given deformation and the number of test cycles. Symmetric or close to symmetric stress cycle is found at relatively high values of the given deformation ε_a = 0.8 to 0.65% and the number of cycles to failure not exceeding $N = 2500$. If the stress cycle deviates from symmetrical, then the slight excess of the tensile stress up to 100 MPa is observed (see Fig. 2d).

The asymmetrical stress cycle is found in the samples at relatively low values of the specified deformation ε_a = 0.5–0.4% and the number of cycles to failure exceeding $N = 2500$. The less the specified deformation and the larger the number of cycles to failure, the more asymmetric is the stress cycle, reaching the minimum values of $R = -0.5$ in the present work.

Table 1. Mechanical properties of the superalloy VZh175 (mean values)

	Test temperature, °C	Tensile strength σ_b, MPa	Yield point $\sigma_{0.2}$, MPa	Elongation δ, %
VZh175	20	1600	1190	14
	650	1530	1080	12

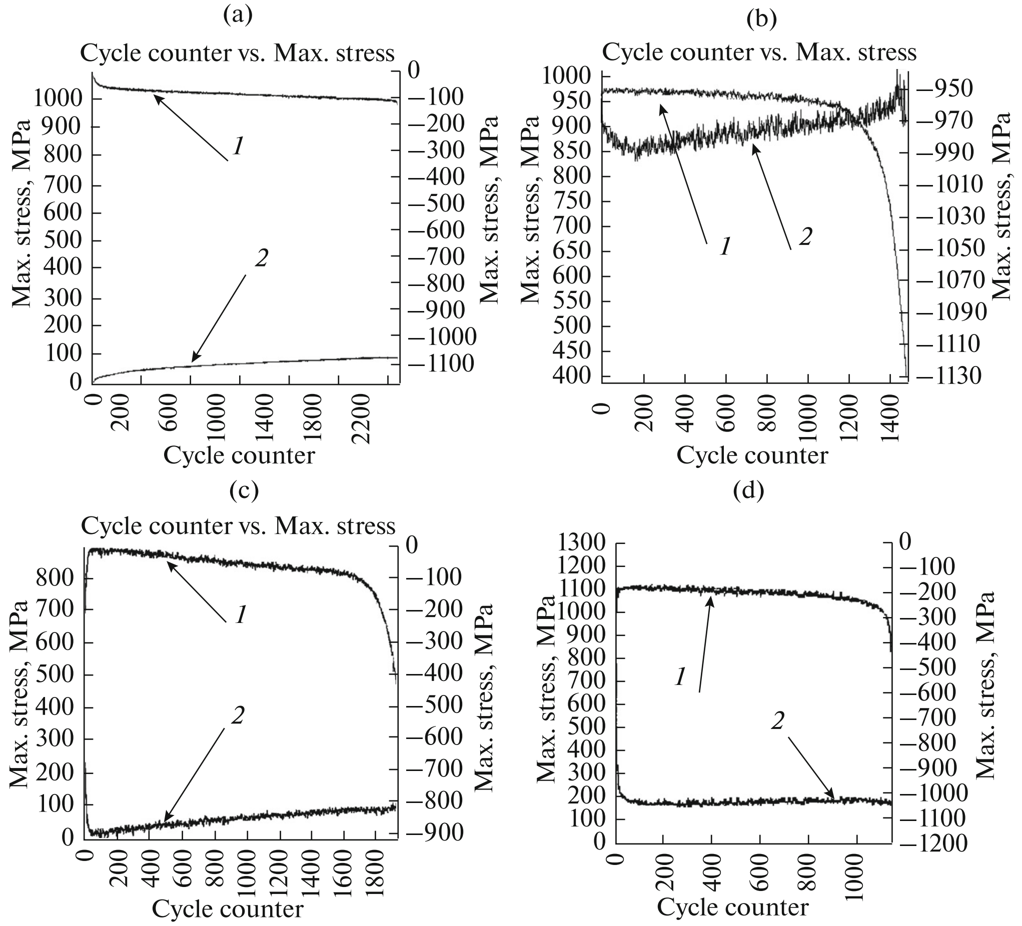

Fig. 2. Change in stresses at given fixed strain: (a) $T = 20°C$, $\varepsilon_a = 0.6\%$, $N_f = 2494$ c.; (b) $T = 650°C$, $\varepsilon_a = 0.6\%$, $N_f = 1486$ c.; (c) $T = 750°C$, $\varepsilon_a = 0.5\%$, $N_f = 1930$ c.; (d) $T = 650°C$, $\varepsilon_a = 0.65\%$, $N_f = 1140$ c. (asymmetry ratio $R_\varepsilon = 0$); (*1*) maximum tensile strength; (*2*) minimum tensile strength.

Another parameter of the cyclic elastoplastic deformation is the width of the hysteresis loop, which characterizes the value of the inelastic deformation ε_{in} accumulated in the material. The ε_{in} parameter does not significantly change during the test at the symmetrical deformation cycle $R = -1$ and at all three test temperatures on the fixed section. However, it varies ambiguously depending on the test temperature at the constancy of such conditions as given deformation ε_a and the number of cycles $N = N_f/2$. The increase in the test temperature from 20 to 650°C causes a decrease in the ε_{in} values, whereas the subsequent increase in temperature up to 750°C leads to an increase in the ε_{in} values. At the amplitude of the given deformation $\varepsilon_a = 0.5\%$ and temperature growth, the ε_{in} parameter has the following values: 0.16, 0.05, 0.11% (Fig. 3).

With the symmetric $R = -1$ and the asymmetric $R = 0$ loading cycles, the values of accumulated stress ε_{in} (at $N = N_f/2$) are fairly close to each other at equal values of the given deformation ε_a (Fig. 4).

Table 2. Mean stresses tensile–compression stresses on the stable part of the stress–number of cycles diagram depending on test temperature

Test temperature, °C	20	650	750
Number of cycles to failure N_f	$N_f \approx 2000$ c.		
Strain amplitude of cycle ε_a, %	0.6	0.6	0.5
Mean stresses of strain–compression σ, MPa	985–1030	900–890	845–850

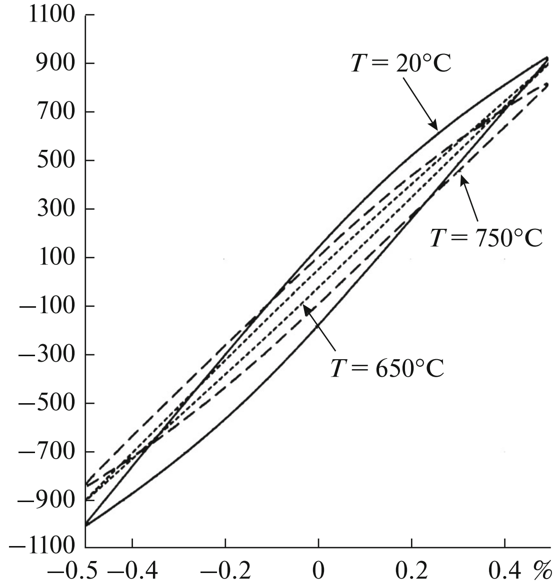

Fig. 3. Influence of test temperature on the parameter ε_{in}, $\varepsilon_a = 0.5\%$, $N = (N_f/2)$, $T = 20°C$, $N = 6500$ c.; $T = 650°C$, $N = 2100$ c.; $T = 750°C$, $N = 1000$ c.

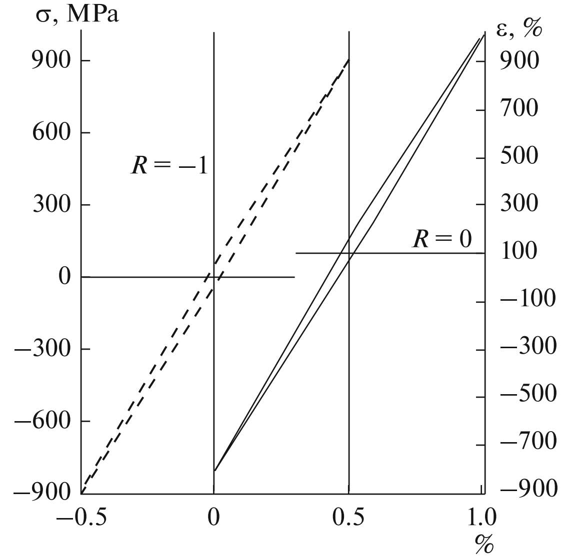

Fig. 4. Influence of the asymmetry ratio R_e on parameters of the elastoplastic hysteresis loop $T = 650°C$, $\varepsilon_a = 0.5\%$: $R = -1$, $N = N_f/2 = 2000$ c., $\varepsilon_{in} = 0.0413\%$; $R = 0$, $N = N_f/2 = 1500$ c., $\varepsilon_{in} = 0.0466\%$.

Study of the low-cycle fatigue (LCF) characteristics of the VZh175 superalloy was carried out along with the study of parameters of cyclic elastoplastic deformation. Procedures of linear regression analysis were applied for processing of the test results. The amplitude of the given deformation ε_a was considered as an independent value, and the logarithm of the number of cycles to failure $\log N_p$ was a dependent random variable. The equation of the middle fatigue line is given in the form $\varepsilon^m N = C$. After taking the logarithm, it takes the form $\log N = a + b\log\varepsilon$, and graphically it is a straight line in double logarithmic coordinates. The coefficients a and b of the equation are determined by the least squares method. In addition to the average LCF values, the characteristics of the $\log N_f$ scatter to failure were determined dispersion S^2 and root mean squared S were determined [19].

Test results of samples of the VZh175 alloy at 20, 650, and 750°C at a symmetric loading cycle $R = -1$ are shown in Fig. 5; at 650°C and two values of asymmetry factor R, in Fig. 6. The LCF limits as concerns deformation and other LCF characteristics of the VZh175 superalloy were determined; they are given in Table 3.

Analysis of the test results for LCF during the symmetrical deformation cycle at $R = -1$ and three indicated temperatures showed that the VZh175 alloy had a higher LCF limit at room temperature. There is a clear tendency toward convergence of the LCF values with the increase in the test base. High values of correlation coefficient r indicate the validity of the linear approximation of test results for LCF under the given test conditions.

On the basis of the test results obtained at 650 and 750°C, the following should be emphasized. In the longevity interval of $N = 2 \times 10^2$– 1.5×10^4 cycles, the line of the average LCF values at 650°C is higher than the LCF line at 750°C; i.e., at a lower temperature, the VZh175 alloy possesses higher values of the fatigue limit. However, the LCF midlines are consistently drawing in, and on the basis of testing for $N = 10^4$ cycles, the difference within LCF is 0.01% and it is minimal. With a slight increase in the test base to $N = 1.5 \times 10^4$ cycles, the LCF lines of average values inter-

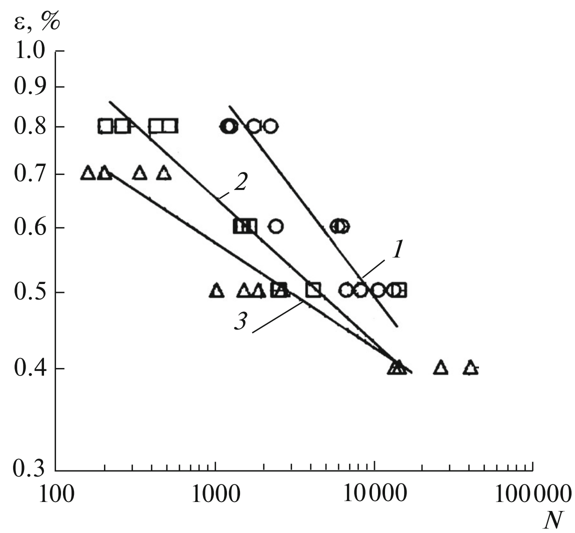

Fig. 5. Low-cycle fatigue of the VZh175 superalloy at test temperatures, °C: (*1*, ○) 20; (*2*, □) 650; (*3*, △) 750.

sect and the LCF limits take equal values. Such correlation of durability characteristics with increasing temperature contradicts the generally observed correlation for superalloys, where the increase in temperature within the operational boundaries leads to a steeper slope of the regression line of superalloys and decrease in the LCF limit. It should be concluded in the present work that the increase in temperature from 650 to 750°C does not exert a significant influence on resistance of the VZh175 superalloy to low cycle fatigue in the longevity area of 10^4 cycles under the specified conditions of the experiment. More specific conclusions concerning the influence of high temperature may be made with the accumulation of new experimental information.

Let us note that a similar result concerning the mutual position of the LCF midlines for the foreign nickel alloys is given in [8, 9].

For LCF midlines, the S values of the logarithm of the number of cycles to failure, $S_{\log N}$, does not show more than a twofold difference (see Table 3). There are no experimental results which differ sharply from the average values of the logarithm of the number of cycles to failure log*N*. Any tendency of the dependence of dispersion S^2 and S on test temperature is not present. The obtained scatter characteristics may be compared with data in the literature for similar composition of the EI698VD superalloy but obtained in a soft cycle of loading and coefficient of asymmetry $R = 0$. For the EI698VD superalloy at 650°C, the value $S = 0.568$ [20], and at 400°C, $S = 0.247$ [21]. Thus, it may be assumed that the VZh175 alloy when tested for LCF under the given deformation is characterized by a small scatter of experimental results.

The influence of cycle asymmetry of deformation on the LCF characteristics of the VZh175 superalloy at 650°C was studied. Investigation of the asymmetrical deformation influence on the LCF characteristics allows approaching determination of the mechanical properties closer to real operational conditions of material in the rotary components. The LCF characteristics determined at the coefficient of asymmetry of the cycle of deformation $R = -1$ (symmetric cycle) and $R = 0$ (asymmetric cycle) were compared. Data presented in Fig. 6 and in Table 3 show that the LCF characteristics have very close values within the entire test interval. On the basis of $N = 10^4$ cycles, the values of endurance limits coincide, $\varepsilon_a = 0.43\%$.

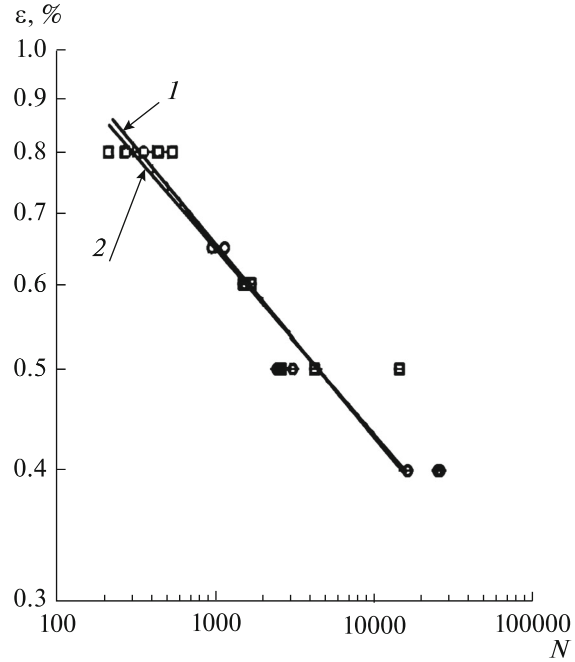

Fig. 6. Influence of the asymmetric deformation on LCF of the VZh175 alloy at test temperature of 650°C: (*1*, □) $R = -1$; (*2*, ○) $R = 0$.

The fracture behavior of specimens tested for LCF at 20, 650, and 750°C and symmetric cycle of deformation $R = -1$ was studied. Samples were tested in the range of deformations of 0.8–0.4%. Similar of fractured surfaces was observed at all these temperatures.

In all cases, the origin of a crack starts from the surface of the sample; the source of fracture, area of the crack growth, and rupture are clearly seen (Fig. 7). At decreasing amplitude of the given deformation, the increase in the crack growth area of the low-cycle fatigue and decrease in the rupture zone are observed. The area of fatigue crack growth increases from 25–30% at $\varepsilon_a = 0.8$ to 70% with $\varepsilon_a = 0.4\%$. The surface of the low-cycle fatigue fracture has a relatively flat mac-

Table 3. LCF characteristics of the VZh175 alloy at room and operating temperatures

Test temperature T, °C	Number of tested samples, n, pcs.	Asymmetry ratio R	LCF limit on the basis of $N_f\varepsilon_a$, %		Coefficients of the regression equation		Correlation ratio r	Scatter characteristics log$N$	
			10^3	10^4	a	b		dispersion S^2	S
20	11	–1	0.90	0.50	2.83	–3.79	–0.92	0.0172	0.131
650	11	–1	0.66	0.43	1.99	–5.49	–0.92	0.0118	0.109
750	12	–1	0.58	0.42	1.17	–7.60	–0.95	0.0468	0.216
650	11	0	0.65	0.43	1.92	–5.72	–0.97	0.0206	0.143

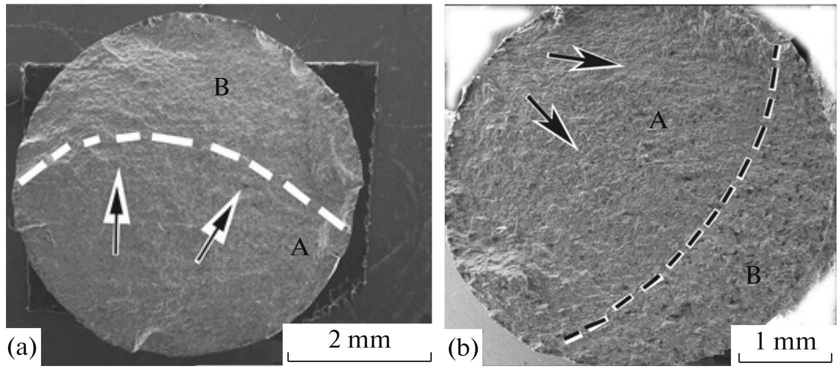

Fig. 7. The fracture surface of VZh175 superalloy samples tested for LCF at given deformation: (a) $T = 20°C$, $\varepsilon_a = 0.6\%$, $N_f = 1536$ c., (A) source of fracture and area of LCF crack propagation, (B) rupture; (b) $T = 750°C$, $\varepsilon_a = 0.4\%$, $N_f = 26\,835$ c, (A) source of fracture and area of LCF crack propagation, (B) rupture.

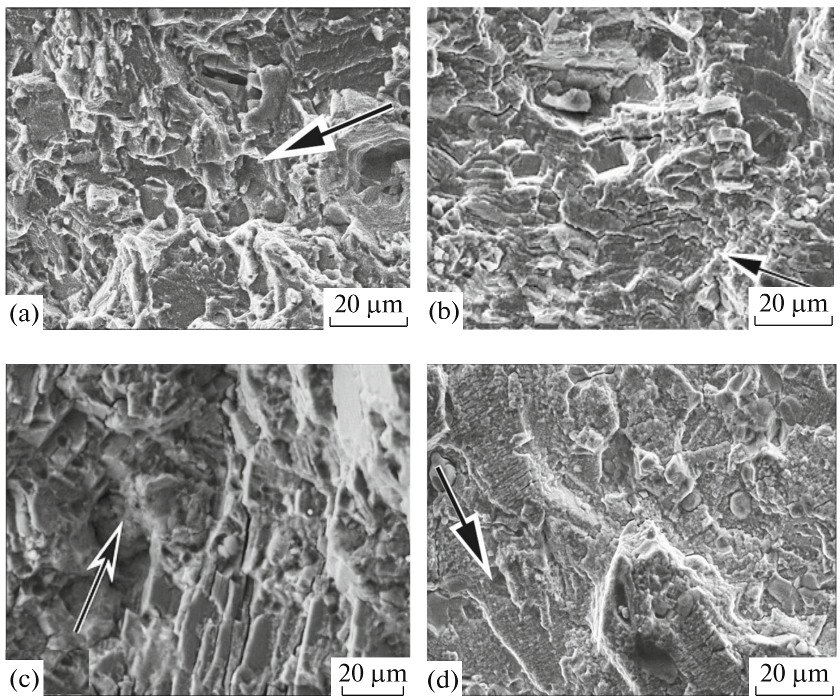

Fig. 8. Fracture surface of the VZh175 superalloy samples at the stage of the LCF crack propagation: (a) $T = 20°C$, $\varepsilon_a = 0.6\%$, $N_f = 6438$ c., ductile fracture behavior with separate parts of the striated relief; (b) $T = 650°C$, $\varepsilon_a = 0.6\%$, $N_f = 1536$ c., ductile fracture behavior, initial stage of the accelerated crack propagation; (c) $T = 750°C$, $\varepsilon_a = 0.4\%$, $N_f = 26835$ c., longitudinal humps toward fatigue crack propagation; (d) $T = 650°C$, $\varepsilon_a = 0.5\%$, $N_f = 8472$ c., striated relief of the surface in the region of the accelerated LCF crack propagation.

rorelief of the surface with the area of the fatigue crack growth (area A) and area of the static rupture (area B).

Figures 8a and 8b show the characteristic areas of the surface fatigue fracture at the stage of the fatigue crack propagation in samples tested at equal values of the deformation amplitude $\varepsilon_a = 0.6\%$ and temperatures of 20 and 650°C. At both temperatures, the fracture surface is relatively flat; it has a heterogeneous, mainly ductile relief, which reflects the heterogeneous structure of the alloy. At 650°C, the secondary cracking of the fracture surface is observed.

Sites with typical fatigue fracture relief are observed in the area of accelerated growth of the LCF crack, closer to the end of the area. It is seen in Figs. 8c and 8d that at high temperatures areas with elongated protrusions with secondary cracking are observed in the direction of the crack propagation. In another case, areas with striations located across the direction of crack propagation, which are typical sign of fatigue fracture, are formed.

CONCLUSIONS

1. During tests for low-cycle fatigue (LCF) of the VZh175 superalloy under given deformation at 20, 650, and 750°C, the single-type charts of change in cyclic stresses, depending on the number of cycles N, that include the longest area of quite stable stresses were implemented.

2. The width of the elastoplastic hysteresis loop ε_{in} on the stable area ambiguously depends on the test temperature if other parameters are constant. When the amplitude of deformation is $\varepsilon_a = 0.5\%$ and $N = N_p/2$, the width of the loop will vary within the interval of $\varepsilon_{in} = 0.16–0.05\%$.

3. The VZh175 superalloy has the highest LCF limit at the symmetrical deformation cycle $R = -1$ at room temperature. At room and high temperatures, the LCF limits converge with the increase in the number of cycles. On the basis of $N = 10^4$ cycles, the values of the test margins are located within the range of $\varepsilon_a = 0.42–0.50\%$. Transition from the symmetric deformation cycle to asymmetric $R = 0$ does not have a significant impact on the LCF limit value.

4. The LCF of the VZh175 alloy at test temperatures specified in the present work is characterized by relatively small values of the scatter of the logarithm of the number of cycles to failure $\log N_f$ relative to the LCF line of the VZh175 alloy corresponding to 50% probability of nonfailure. The root mean squared value S is accepted as the evaluation criterion. Any tendency of dependence of dispersion S^2 and S on the test temperature is not present.

5. The character of the fracture behavior of samples tested under conditions of low-cycle deformation was studied. The origin of cracks in all cases begins from the surface of samples. Macro fracture of the fractured surface is relatively flat with a well-pronounced propagation area of the fatigue crack. There are certain differences in the character of fracture depending on temperature. Rough and uneven relief is observed in the zone of fatigue crack growth at room temperature; fatigue striations occupy a small part of the surface and are located in the area of accelerated crack growth closer to the rupture. Uneven relief is also observed at high test temperatures in the initial stage of crack growth. However, with the crack propagation, the fracture surface becomes flatter; striated relief and microcracking are formed on part of the surface.

ACKNOWLEDGMENTS

This work was performed under support of the Russian Foundation for Basic Research (grant no. 13-08-12084).

REFERENCES

1. Inozemtsev, A.A., Ratchiev, A.M., Nikhamkin, M.Sh., et al., Low-cycle fatigue and cyclic crack resistance of a nickel alloy under loading specific for turbine disks, *Tyazh. Mashinostr.*, 2011, no. 4, pp. 30–33.
2. Kablov, E.N., Innovative developments of the All-Russian Scientific Research Institute of Aviation Materials within the project "Strategic development of materials and technologies of their recycling until 2030," *Aviats. Mater. Tekhnol.*, 2015, no. 1, pp. 3–33.
3. Terent'ev, V.F., *Ustalost' metallicheskikh materialov* (Fatigue of Metal Materials), Moscow: Nauka, 2003.
4. Reed, R.C., *The Superalloys: Fundamentals and Applications*, Cambridge: Cambridge Univ. Press, 2006.
5. Gorbovets, M.A., Bazyleva, O.A., Belyaev, M.S., and Khodinev, I.A., Low-cycle fatigue of VKNA type single-crystal intermetallic alloy under "hard" loading conditions, *Metallurgist*, 2014, vol. 58, nos. 7–8, pp. 724–728.
6. Belyaev, M.S., Terent'ev, V.F., Gorbovets, M.A., Bakradze, M.M., and Antonova, O.S., Low-cycle fatigue of a high-temperature nickel alloy VZh175 under hard loading, *Deform. Razrushenie Mater.*, 2015, no. 9, pp. 17–24.
7. Golubovskiy, E.R., Svetlov, I.L., Petrushin, N.V., Cherkasova, S.A., and Volkov, M.E., Low-cycle fatigue of nickel superalloy single crystals at elevated temperatures, *Russ. Metall.* (Engl. Transl.), 2010, vol. 2010, no. 8, pp. 941–947.
8. Wright, J.K., Carroll, L.J., Simpson, J.A., et al., Low cycle fatigue of alloy 617 at 850°C and 950°C, *J. Eng. Mater. Technol.*, 2013, vol. 135, no. 7, pp. 031005 (1-8).
9. Zhong, Z., Gu, Y., Yuan, Y., et al., On the low cycle fatigue behavior of a Ni-based superalloy containing high Co and Ti contents, *Mater. Sci. Eng., A*, 2012, vol. 552, pp. 434–443.
10. Gao, G., Duan, S., and Zhang, W., A study of high temperature low cycle fatigue life prediction for two superalloys, *J. Eng. Res.*, 2015, vol. 3, no. 1, pp. 114–126.
11. Gao, G., Duan, S., and Zhang, W., Low cycle fatigue life prediction for GH 4133 at 550°C based on power-exponent function, *J. Eng. Res.*, 2015, vol. 3, no. 3, pp. 111–124.
12. Maier, G., Riedel, H., and Somsen, C., Cyclic deformation and lifetime of alloy 617B during isothermal low cycle fatigue, *Int. J. Fatigue,* 2013, vol. 55, pp. 126–135.
13. Kablov, E.N., Ospennikova, O.G., Lomberg, B.S., and Sidorov, V.V., Advanced technologies for the production of heat-resistant materials for aircraft engine manufacturing, *Probl. Chern. Metall. Materialoved.*, 2013, no. 3, pp. 47–54.
14. Lomberg, B.S., Ovsepyan, S.V., Bakradze, M.M., et al., High temperature heat resistant nickel alloys for gas turbine engine parts, *Aviats. Mater. Tekhnol.*, 2012, suppl., pp. 52–57.
15. Bakradze, M.M., Ovsepyan, S.V., Shugaev, S.A., and Letnikov, M.N., Effect of quenching on the structure

and properties of forgings from the nickel heat-resistant alloy EK151-ID, *Tr. Vseross. Inst. Aviats. Mater.*, 2013, no. 9, art. 01. http://www.viamworks.ru. Accessed February 12, 2015.

16. Lomberg, B.S., Ovsepyan, S.V., and Bakradze, M.M., Specific alloying and heat treatment of high-temperature nickel alloys for the discs of new generation gas turbine engine, *Aviats. Mater. Tekhnol.,* 2010, no. 2, pp. 3–8.

17. Kablov, E.N., Ospennikova, O.G., and Lomberg, B.S., Complex innovative technology of isothermal stamping in air in superplasticity mode of disks made of superheat resistant alloys, *Aviats. Mater. Tekhnol.,* 2012, suppl., pp. 117–129.

18. Kablov, E.N., Petrushin, N.V., Svetlov, I.L., and Demonis, I.M., New nickel casted heat-resistant alloys, *Aviats. Mater. Tekhnol.*, 2012, suppl., pp. 36–51.

19. Stepnov, M.N. and Shavrin, A.V., *Statisticheskie metody obrabotki rezul'tatov mekhanicheskikh ispytanii: spravochnik* (Statistical Data Processing of the Results of Mechanical Tests: Handbook), Moscow: Mashinostroenie, 2005.

20. Golubovskii, E.R., Volkov, A.S., Volkov, S.N., et al., Characteristics of the constructional strength (low-cycle fatigue and crack growth rate due to fatigue) of the metal stampings of disks made of the EI698VD alloy produced by Ruspolimet Company, *Aviats.-Kosm. Tekh. Tekhnol.*, 2010, no. 9, pp. 82–86.

21. Velikanova, N.P., Statistical analysis of experimental study results on low-cycle fatigue resistance for the EI698-VD high-temperature alloy, *Russ. Aeronaut.*, 2009, vol. 52, no. 4, pp. 413-418.

Translated by E. Grishina